Biochimica et Biophysica Acta, 979 (1989) 166–176
Elsevier

BBA 74326

Intrinsic molecules in lipid membranes change the lipid-domain interfacial area: cholesterol at domain interfaces

Leonor Cruzeiro-Hansson [1], John Hjort Ipsen [2] and Ole G. Mouritsen [2]

[1] *Laboratory of Applied Mathematical Physics and* [2] *Department of Structural Properties of Materials, The Technical University of Denmark, Lyngby (Denmark)*

(Received 30 August 1988)

Key words: Lipid bilayer; Phase transition; Interface active molecule; Cholesterol; Density fluctuation; Heterogeneity; Lateral compressibility

A theoretical analysis of the effects of intrinsic molecules on the lateral density fluctuations in lipid bilayer membranes is carried out by means of computer simulations on a microscopic interaction model of the gel-to-fluid chain-melting phase transition. The inhomogeneous equilibrium structures of gel and fluid domains, which in previous work (Cruzeiro-Hansson, L. and Mouritsen, O.G. (1988) Biochim. Biophys. Acta 944, 63–72) were shown to characterize the transition region of pure lipid membranes, are here shown to be enhanced by intrinsic molecules such as cholesterol. Cholesterol is found to increase the interfacial area and to accumulate in the interfaces. The interfacial area, the average cluster size, the lateral compressibility, and the membrane area are calculated as functions of temperature and cholesterol concentration. It is shown that the enhancement by cholesterol of the lateral density fluctuations and the lipid-domain interfacial area is most pronounced away from the transition temperature. The implications of the results are discussed in relation to passive ion permeability and function of interfacially active enzymes such as phospholipase.

Introduction

It is well-known experimentally [1] as well as theoretically [2] that molecules which are intrinsically incorporated in lipid bilayer membranes have a significant effect on the macroscopic phase equilibria and the lateral organization of the mixed system. This is particularly true of integral proteins, which almost invariably lead to massive phase separation [3]. In the case of cholesterol, the effects are more subtle in that only a very narrow phase separation region is observed up to about 10 mol%, beyond which massive phase separation sets in [4–7]. In contrast to the macroscopic phase equilibria, much less is known quantitatively about the actual microscopic lateral distribution of intrinsic molecules in lipid membrane phases. This lack of information is particularly striking with regard to the lateral molecular distribution in transition regions where lipid membranes are known to be significantly influenced by strong lateral density fluctuations, leading to equilibrium inhomogeneous domain structures in the membrane [8–13]. This is a very difficult problem to approach experimentally and, in most cases, the lateral distribution has to be inferred indirectly from measurements of bulk physical properties. Theoretically this is not an easy problem either, since it is hard to analyze theoretical models in terms of heterogeneous states and thermal density fluctuations.

In this paper we describe the results of a theoretical study of the effects of small intrinsic molecules on lipid membrane fluctuations and interfacial properties. We shall pay particular attention to hydrophobically smooth intrinsic molecules, such as cholesterol. The study involves computer simulations on a microscopic model which accounts for the lipid–lipid as well as lipid–intrinsic molecule interactions. The work is a natural extension of our recent study of the temperature variation of the lipid-domain interfacial area in pure lipid bilayers and its relation to passive transmembrane ion permeability [14]. Computer simulations not only allow macroscopic thermodynamic properties, such as phase equilibria, lateral compressibility, specific heat and membrane area, to be calculated, but also give direct

Abbreviations: DPPC, dipalmitoylphosphatidylcholine; DMPC, dimyristoylphosphatidylcholine.

Correspondence: O.G. Mouritsen, Department of Structural Properties of Materials, The Technical University of Denmark, Building 307, DK-2800 Lyngby, Denmark.

access to the microstructure of the membrane system [15]. Hence, information about clusters, interfaces and lateral distribution of the intrinsic molecules can readily be calculated. This is particularly advantageous regarding the interpretation of indirect experimental measurements of membrane organization and its relationship to membrane function.

Model of phase transition and interactions between lipids and intrinsic molecules

As the underlying microscopic model of the pure lipid membrane gel-to-fluid phase transition we have adopted the ten-state model of Pink and collaborators [16]. This model takes full account of the acyl-chain conformational statistics as well as the van der Waals interactions between the various conformers. The model has been useful in analyzing bulk thermodynamic and spectroscopic data for pure lipid bilayers [17,18] as well as for protein- and cholesterol-containing bilayers [4,18–21]. This paper describes the first use of the model to quantitatively study the influence of intrinsic molecules, such as small proteins and cholesterol, on the membrane fluctuations and lateral organization.

In the ten-state model [16], it is the conformational acyl-chain states and their statistics that are responsible for the gel-to-fluid phase transition, which is predominantly a chain-melting transition [22]. The model incorporates ten conformational states, of which one is the fully ordered all-*trans* conformation and one is a highly excited fluid state, which is characteristic of the high-temperature thermodynamic fluid phase (f). The eight remaining states correspond to intermediate chain conformations, which together with the all-*trans* state are characteristic of the thermodynamic low-temperature gel phase (g). Each of the ten states, n, is described by a cross-sectional area, $A_{\mathrm{L}n}$, an internal energy, $E_{\mathrm{L}n}$, and an internal degeneracy, $D_{\mathrm{L}n}$. The values of the various model parameters are the same as those used in our previous study of the lipid-domain interfacial area in the ten-state model of pure DPPC bilayers [14].

We shall here model the interactions between the lipid molecules and the intrinsic molecules (for convenience hereafter called cholesterol) in the simplest possible setting by assuming that cholesterol is a stiff, hydrophobically smooth molecule with no internal degrees of freedom. The molecule is assigned a cross-sectional area, $A_{\mathrm{C}} = 32$ Å^2 [23]. In the spirit of the form of lipid–lipid interaction, which is given in terms of shape-dependent nematic chain-order parameters, $I_{\mathrm{L}n}(A_{\mathrm{L}n})$, cholesterol is assigned a shape factor, I_{C}, which, however, is constant. I_{C} is related to the van der Waals interaction between the hydrophobic part of the cholesterol molecule and the corresponding part of a lipid chain or another cholesterol molecule. Consequently, the total Hamiltonian of the cholesterol-lipid bilayer becomes

$$H = \sum_{i}\sum_{n=1}^{10}(E_{\mathrm{L}n} + \Pi A_{\mathrm{L}n})\mathscr{L}_{ni} + \Pi A_{\mathrm{C}}\sum_{i}\mathscr{L}_{\mathrm{C}i}$$

$$-\frac{J_0}{2}\sum_{i,j}\sum_{n,m=1}^{10} I_{\mathrm{L}n}I_{\mathrm{L}m}\mathscr{L}_{ni}\mathscr{L}_{mj}$$

$$-\frac{J_0}{2}\sum_{i,j}\sum_{n=1}^{10} I_{\mathrm{L}n}I_{\mathrm{C}}(\mathscr{L}_{ni}\mathscr{L}_{\mathrm{C}j} + \mathscr{L}_{nj}\mathscr{L}_{\mathrm{C}i}) - \frac{J_0}{2}\sum_{i,j} I_{\mathrm{C}}^2\mathscr{L}_{\mathrm{C}i}\mathscr{L}_{\mathrm{C}j} \qquad (1)$$

In Eqn. 1, J_0 is the strength of the van der Waals interactions. $\mathscr{L}_{ni}$ and $\mathscr{L}_{\mathrm{C}i}$ are the occupation variables ($= 0, 1$) of lipid and cholesterol molecules, respectively, and Π is an internal lateral pressure which assures bilayer stability. The cholesterol concentration is given as $x_{\mathrm{C}} = \langle\mathscr{L}_{\mathrm{C}i}\rangle/(2 - \langle\mathscr{L}_{\mathrm{C}i}\rangle)$.

The model, Eqn. 1, of the mixed system contains only one new parameter, I_{C}, relative to the pure lipid bilayer model. I_{C} is determined by the requirement that the phase diagram resembles that of phosphatidylcholine/cholesterol mixtures for x_{C} up to about 10%, i.e., with a very narrow coexistence region and a modest freezing-point depression [4,5]. A simple mean-field calculation suggests $I_{\mathrm{C}} = 0.45$ to be a suitable choice. It should be noted, however, that Eqn. 1 is not a realistic model of lipid/cholesterol mixtures beyond 8–10 mol%, where phase separation sets in between either gel or fluid lipid phases and a peculiar phase of high-cholesterol content which is fluid but at the same time has lipid chains of high conformational order [4,5]. In a more realistic model, these peculiar properties of the phase diagram are ascribed to a subtle balance between the limited solubility of cholesterol in the solid gel phase and its preference of ordered acyl chains [4]. This subtlety is neglected in the present work.

We have used Monte Carlo computer simulation techniques [15] to determine numerically the statistical mechanical and thermodynamic properties of the model in Eqn. 1 with an annealed dilution of cholesterol. The simulations are carried out on triangular lattices of different sizes subject to periodic boundary conditions. The results presented below are obtained mainly for a lattice of 100^2 sites. Finite-size analyses show that systems of this size represent the thermodynamic limit as far as the properties considered in this paper are concerned. Lipid and cholesterol molecules occupy two and one lattice sites, respectively. Equilibrium for the present model is provided by a combination of Glauber and Kawasaki dynamics [15]. The Glauber dynamics refer to single-chain excitations. Kawasaki dynamics, conserving the cholesterol concentration, refer to pair exchange of lipid chains and cholesterol molecules.

Phase diagram, membrane area and lateral compressibility

The phase diagram derived from a mean-field calculation for $I_C = 0.45$ is shown as an inset in Fig. 1. It is seen that the coexistence region is very narrow and there is a modest freezing-point depression. The diagram is terminated by a critical end-point at $x_C \approx 0.48$. The phase diagram has been scanned in temperature by computer simulation for $x_C = 0$, 0.04, 0.08, 0.12, 0.25 and 0.50. The two higher concentrations are included in the study for the sake of completeness. We do not expect that the results for these concentrations are relevant in the case of cholesterol-containing membranes.

The average cross-sectional area, A, per molecule of the mixture is shown in Fig. 1. It is noted that the transition is broadened by the presence of cholesterol and at most temperatures A decreases as x_C increases. In a temperature region below the transition there is, however, a more ocmplicated relationship between A and x_C. A more clear picture of the effect of cholesterol on the lipid membrane is obtained by suppressing the mere dilution effect on A. For that purpose, we have in Fig. 2 plotted the cross-sectional area per lipid molecule, $A_L = (A - x_C A_C)/(1 - x_C)$, which clearly shows the expected systematic expansion effect of cholesterol below the transition and a similar systematic condensation effect above the transition. This behaviour is also reflected in the microscopic variables which show that below the transition, cholesterol has a disordering effect on the acyl chains and above the transition, the acyl chains become more conformationally ordered as

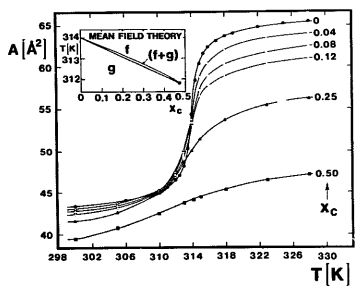

Fig. 1. Cross-sectional area, A, per molecule of the mixture plotted versus temperature for different cholesterol concentrations, x_C. The inset shows the phase diagram as calculated by mean-field theory. The gel and fluid phases are denoted by g and f and the coexistence region by $(g+f)$. The heavy dot denotes a critical end-point in the phase diagram.

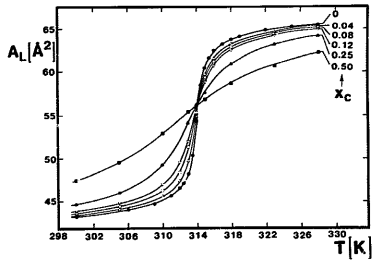

Fig. 2. Cross-sectional area, A_L, per lipid molecule versus temperature for different cholesterol concentrations, x_C.

the cholesterol content increases. It should be emphasized that the effect of cholesterol on A_L seen in Fig. 2 is a significant result, since the simple lipid–cholesterol interaction in Eqn. 1 is nonspecific and operates only on the level of hydrophobic contact interactions.

The isothermal lateral compressibility,

$$\chi(T) = -\left(\frac{\partial A}{\partial \Pi}\right) = (k_B T)^{-1}(\langle A^2\rangle - \langle A\rangle^2) \qquad (2)$$

which in the computer simulations is readily calculated via the fluctuation theorem, is displayed in Fig. 3. $\chi(T)$ is a direct bulk measure of the lateral density fluctuations. The pronounced peak in $\chi(T)$ signals the chain-melting transition, which in the pure system is strongly influenced by thermal fluctuations [11]. The peak height

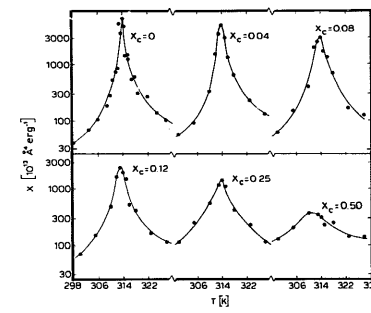

Fig. 3. Semi-logarithmic plot of the isothermal lateral compressibility, $\chi(T)$, Eqn. 2, versus temperature for different cholesterol concentrations, x_C.

is reduced as x_C is increased. Concomitantly, the compressibility function broadens, which implies that, whereas the fluctuations are suppressed near the phase transition by the presence of cholesterol, there is an enhancement of the fluctuations away from the transition! This is a remarkable effect. The same effect is observed for another fluctuation quantity, the specific heat.

Since we observe no signs of a phase separation within the resolution limits of the computer simulation, we can associate the peak position of $\chi(T)$ with the transition point. It is then seen that the simulation results for the transition temperature are in close agreement with the mean-field phase diagram of Fig. 1. We have not attempted to locate the critical end-point by the simulations. However, our results are consistent with the critical point being somewhere in between $x_C = 0.25$ and 0.50.

Heterogeneous membrane structure and cluster sizes

The microscopic phenomena which accompany the strong lateral density fluctuations near the phase transition are illustrated in Fig. 4, which gives a series of snapshots of the microconfiguration at $T = 312$ K for different cholesterol contents. In agreement with our previous results for the pure system [10,11,14], it is observed that the lateral density fluctuations near the phase transition lead to an instantaneous heterogeneous membrane structure where different domains can be discerned. Below the transition, clusters of the fluid phase are formed in the equilibrium gel phase; above the transition, clusters of the gel phase are formed in the equilibrium fluid phase. These clusters (or domains) are not static entities but fluctuate in space and time. As the temperature approaches the transition temperature, cluster formation becomes more dominant and the lateral organization of the membrane becomes very heterogeneous.

It is clear from Fig. 4 that the presence of cholesterol induces larger and more ramified clusters. Furthermore, cholesterol also seems to lead to clustering of the clusters themselves and the resulting superclusters appear to be 'glued' together by locally elevated levels of cholesterol. The superclustering effect becomes more pronounced as x_C is increased. Even more striking is the qualitative observation from Fig. 4 that the cholesterol molecules have a tendency to cluster themselves and moreover to accumulate at the interface between the lipid clusters and the background phase. Hence the overall cholesterol distribution in the plane of the membrane is at any given time not random. We shall quantify this statement in the next section.

The lateral distribution of clusters is described by an equilibrium cluster-size distribution function, $n_l^\alpha(T, x_C)$ [11], $\alpha = g, f$, which we have calculated. n_l^α denotes the number of α-clusters with l lipid molecules. For convenience we have excluded the cholesterol molecules in the cluster-size measure. The average cluster size, $\bar{l}$, is then obtained as

$$\bar{l}(T, x_C) = \sum_{l \geq l_<} l n_l^\alpha(T, x_C) / \sum_{l \geq l_<} n_l^\alpha(T, n_C) \qquad (3)$$

where $\alpha = f$ in the gel phase and $\alpha = g$ in the fluid phase. In the summations of Eqn. 3 we have introduced a lower cut-off in cluster size, $l_<$, to exclude very small 'clusters' [11]. In Fig. 5 we present the results for $\bar{l}(T, x_C)$. The figure shows that the sharp peak in $\bar{l}$ for the pure system [14] loses its intensity in the centre as x_C is increased. The position of the centre remains close to

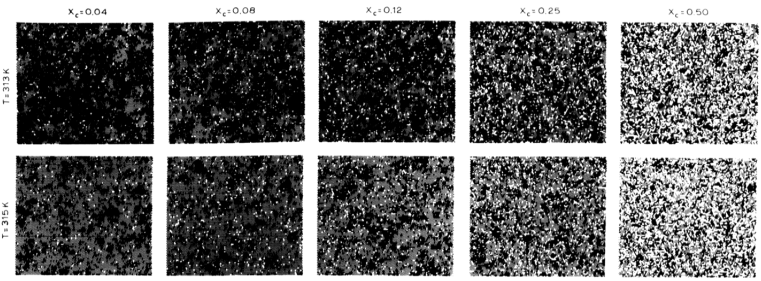

Fig. 4. Snapshots of microconfigurations typical for $T = 313$ and 315 K for a series of cholesterol concentrations, x_C. The system contains $N = 100^2$ lattice sites and hence $(1-x)N/(2-x)$ and $xN/(2-x)$ lipid and cholesterol molecules, respectively. The fluid clusters at $T = 313$ K appear as grey regions on the black background of the gel phase. At $T = 315$ K, the gel clusters appear as black regions on the grey background of the fluid phase. The cholesterol molecules are denoted by blank sites.

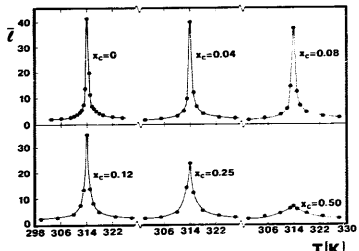

Fig. 5. Average cluster size, $\bar{l}(T, x_C)$ Eqn. 3, as a function of temperature and cholesterol concentration, x_C. $\bar{l}$ denotes the number of lipid molecules in the average-sized cluster. The lower cut-off in this figure is chosen to be $l_< = 3$ lattice sites, i.e., three acyl chains. As discussed in Ref. 14 the effect of increasing $l_<$ is to narrow the peak in $\bar{l}$.

the transition for all concentrations. As $\bar{l}$ decreases close to the transition, there is a concomitant increase of $\bar{l}$ away from the transition. This is a rather remarkable result which, in analogy with the results for the lateral compressibility and the specific heat, suggest that cholesterol enhances the fluctuations and the cluster-formation phenomena in the wings of the transition. However, closer inspection of Fig. 5 shows that such an enhancement takes place only up to a certain cholesterol concentration somewhere above $x_C = 0.25$. At $x_C = 0.50$, the average cluster size has come down again. This is another indication that the critical end-point, cf. Fig. 1, is in between these two concentrations.

Interfacial area and lateral distribution of cholesterol

In order to provide a quantitative characterization of the membrane lateral organization we have divided the membrane area into three regions: the bulk, the clusters, and the interface between the clusters and the bulk. Ambiguities in the measure of the interfacial area are avoided by defining the interface as the set of lattice points in the model which confines the clusters. This definition conforms with that used in Ref. 14 for the first interfacial layer. A second interfacial layer may similarly be defined by those lattice points which constitute the confinement of the cluster plus the first interfacial layer. The interfacial area is then simply taken as the sum of the areas of the lipid acyl chains and cholesterol molecules which occupy the lattice sites of the first interfacial layer.

The conspicuous effects of cholesterol on the interfacial area and the lateral heterogeneity of the membrane are illustrated qualitatively in Fig. 6. This figure shows as a function of cholesterol concentration and temperature how dramatically cholesterol induces larger and more ramified clusters on both sides of the transition. Cholesterol's peculiar effect of inducing clusters of clusters is also evident from Fig. 6, an effect which clearly is enhanced as x_C is increased. A careful inspection of the shapshots in Fig. 6 also reveals the tendency for cholesterol to accumulate in the lipid-domain interfaces. These somewhat qualitative statements will be quantified in the following.

This partitioning of the membrane is most conveniently described quantitatively by the relative amounts of the membrane area in the three regions, specifically the fractional areas, a_b, a_c and a_i of the bulk, the clusters and the interface. Fig. 7 shows the fractional interfacial area, a_i, as a function of temperature for different cholesterol concentrations *. We observe that a_i has a pronounced maximum slightly above the phase transition **. Furthermore, as x_C is increased, there is a monotonic increase in a_i for all temperatures. This finding of an increase in the interfacial area as cholestrol is introduced in the lipid bilayer system is the main result of the present paper. Similar to the fractional interfacial area, also the fractional cluster area, a_c in Fig. 7, exhibits a maximum near the transition and a_c increases for all temperatures as x_C is increased. Concomitantly with the maxima in a_i and a_c the fractional bulk area, a_b in Fig. 7, has a compensating minimum near the transition. The quantities a_b, a_c, and a_i are important for calculations of the passive ion permeability.

The fractional interfacial area in Fig. 7 has contributions from lipid as well as cholesterol molecules. These two contributions, a_{iL} and a_{iC}, are presented separately in Figs. 8 and 9. These figures show that, at the transition for low cholesterol concentrations, there is hardly any change in a_{iL} when cholesterol is introduced, whereas a_{iL} increases steadily with x_C at temperatures away from the transition. In contrast, a_{iC} increases with x_C at all temperatures.

This is a noteworthy set of results which show that cholesterol increases the lipid-domain interfacial area and that the lipid part of this increase is most dramatic away from the transition region. This is clearly demon-

* For the interfacial measures we have in the cluster definition adopted a lower cut-off of $l_< = 14$ chains corresponding to seven lipid molecules in, for example, a hexagon. This somewhat arbitrary choice conforms with the choice of Ref. 14 and facilitates comparison with previous results.

** There is no reason to expect that a_i should peak right at the transition, since there is not a $g \leftrightarrow f$ symmetry in the ten-state model and the g and f cluster distribution functions do not become identical as the transition is approached from either side [11,14].

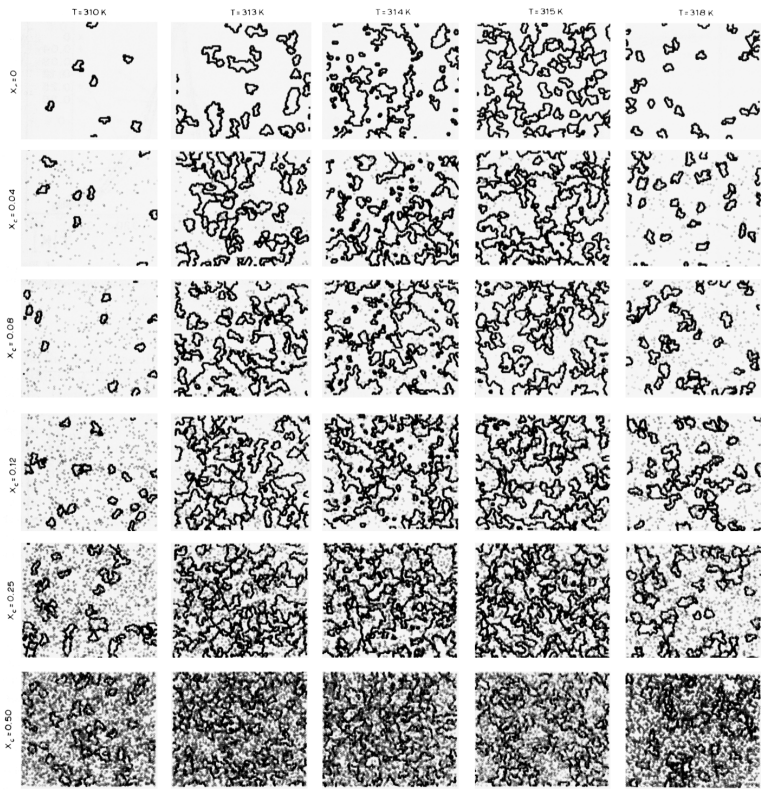

Fig. 6. Snapshots of microconfigurations typical of a variety of cholesterol concentrations, x_C, and temperature. Only the interfacial regions (the solid network) and the cholesterol distribution (○) are shown.

strated in Fig. 10, which shows the excess fractional interfacial area

$$a_{iL}^{excess}(x_C) = a_{iL}(x_C) - a_{iL}(x_C = 0) \quad (4)$$

which simply measures the change due to cholesterol in the lipid part of the interfacial area relative to the pure system. The characteristic dip in a_{iL}^{excess} in the transition region will have important consequences for membrane phenomena which proceed via lipid molecules at interfaces. We shall return to this in the next section when we discuss the influence of cholesterol on passive ion diffusion across membranes.

It is obvious from the results presented in this section, see Figs. 7–10, that the membrane heterogeneity is altered when cholesterol is introduced into the system. At any given time, the cholesterol molecules are not

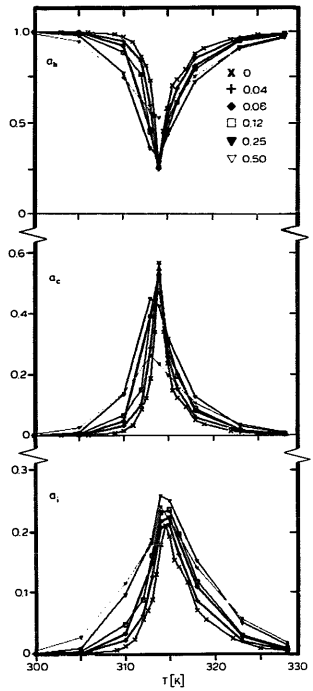

Fig. 7. Fractional bulk area, a_b, fractional cluster area, a_c, and fractional interfacial area, a_i, as a function of temperature for different cholesterol concentrations, x_C.

randomly distributed in the membrane, but there is a clear tendency for cholesterol to accumulate in the interfacial region. This tendency is substantiated in Fig. 11, which gives the results for the ratio between the cholesterol concentration in the interface and the cholesterol concentration in the bulk. The level of cholesterol in the interfaces is more than twice that of cholesterol in the bulk. Fig. 11 also shows that there is a slight decrease of this ratio as x_C is increased and that the ratio also seems to decrease slightly with temperature.

Finally, we have analyzed the second interfacial layer and found that the properties of this layer are the same

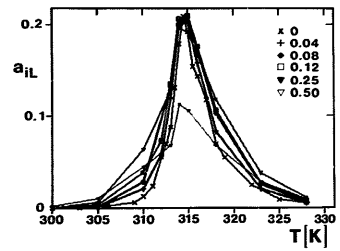

Fig. 8. Lipid part, a_{iL}, of the fractional interfacial area, a_i, cf. Fig. 7, as a function of temperature for different cholesterol concentrations, x_C.

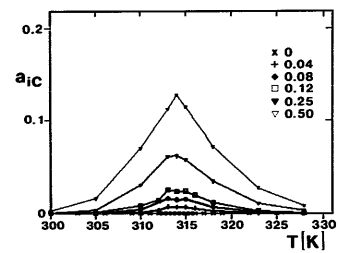

Fig. 9. Cholesterol part, a_{iC}, of the fractional interfacial area, a_i, cf. Fig. 7, as a function of temperature for different cholesterol concentrations, x_C.

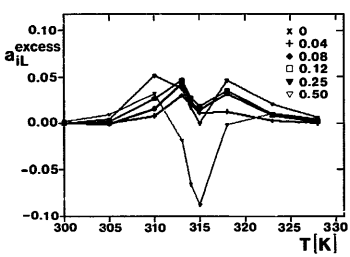

Fig. 10. Excess fractional interfacial area, a_{iL}^{excess} in Eqn. 4, of the lipid part of the interface as function of temperature and cholesterol concentration, x_C.

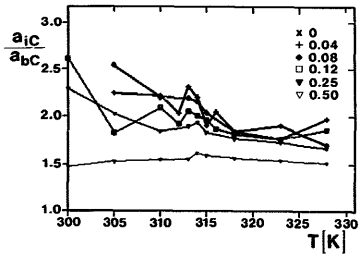

Fig. 11. Ratio, a_{iC}/a_{bC}, between the cholesterol concentration in the interfaces and the cholesterol concentration in the bulk for different global cholesterol concentrations, x_C.

as in the bulk. Specifically, the local cholesterol concentration is down to that characteristic of the bulk phase. Hence, we conclude that the special interfacial properties are sharply localized to basically a single molecular layer.

It should be pointed out that the heterogeneous and highly non-random distribution of cholesterol described in this section only exists on a time scale corresponding to the lifetime, τ, of the average cluster. If the membrane system is observed on time-scales which are much longer than τ, the membrane organization will appear as homogeneous.

Membrane phenomena at lipid-domain interfaces: passive ion permeability

There are a number of examples of membrane phenomena which are believed to take place in association with lipid-bilayer density fluctuations and the formation of lipid-domain interfacial regions. Among these phenomena are passive permeation of for example, ions and molecules [14,24–28] and activity of certain membrane-bound enzymes [29], such as phospholipase [30–32]. These functional processes exhibit a variation with temperature which closely resembles that of the average cluster size, Eqn. 3, or the specific heat [8,14]. It is obvious that interface-active intrinsic molecules, such as the one studied in the present work, which change the interfacial area, must influence the membrane phenomena controlled by density fluctuations and which take place in the interfacial region.

The passive permeability of small ions, such as Na^+, is a phenomenon which has been related to the interfacial area [14,24,25,27]. In a recent analysis [14] we showed that the experimental finding of a sharp peak in the Na^+ permeability at the phase transition of pure lipid bilayers can be rationalized via the temperature variation of the fractional interfacial area, cf. Fig. 7 at $x_C = 0$. This analysis was built on a kind of minimal model for ion permeability, which assumed that the fractional areas, a_b, a_c and a_i are associated with different regional probabilities of transfer, p_b, p_c, and p_i, $p_i \gg p_b$, p_c. The probabilities of transfer are assumed to be independent of temperature so the temperature-dependence remains solely with the fractional areas. Here we shall generalize this model to apply to membranes with intrinsic molecules, such as cholesterol, by writing the probability, $P(T, x_C)$, of an ion crossing the membrane as

$$P(T, x_C) = a_b(T, x_C)p_b + a_c(T, x_C)p_c + a_{iL}(T, x_C)p_i + a_{iC}(T, x_C)p_{iC} \quad (5)$$

In Eqn. 6 we have introduced a special regional probability of transfer, p_{iC}, associated with cholesterol in the interface. For simplicity we shall assume that $p_{iC} = p_b$ below the phase transition. Hence, there are no new parameters to be determined relative to the model for pure lipid bilayers. The values of p_b, p_c, and p_i are taken to be the same as those used for the pure system [14].

To facilitate a direct comparison between the theoretical predictions for the passive ion permeability, we calculate the quantity [14]

$$R'(T, x_C) = A(T, x_C)^{-1/2}T^{1/2}P(T, x_C) \quad (6)$$

which we shall refer to as the reduced permeability. R' is proportional to the logarithm of the fraction of ions which would be retained in a liposome, cf. Ref. 14. Since the full expression for the permeability involves some unknown constants, which usually are avoided in the comparison with experiments by taking the ratio of permeability at some temperature relative to that of some fixed temperature [14,24], we are unable to compare the theoretical results for different values of x_C via

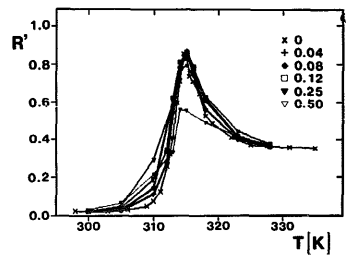

Fig. 12. Reduced permeability, $R'(T)$ Eqn. 6, of Na^+ ions in liposomes as a function of temperature and cholesterol concentration, x_C. $R'(T)$ is given in arbitrary units.

R' and, at the same time, perform a comparison with experimental results. Since there are no available data for ion permeability in membranes with low cholesterol content, we present our data in terms of R', Eqn. 6, and refer to Ref. 14 for a comparison with the experimental results in the case of a pure lipid membrane.

In Fig. 12 are given the theoretical data for the reduced ion permeability $R'(T, x_C)$. We note that R' has a sharp peak near the transition temperature. The centre intensity does not change very much with x_C, whereas the intensity away from the transition increases as x_C is raised. This behaviour simply reflects the variation of the lipid part of the fractional interfacial area in Fig. 8. Hence, we conclude that cholesterol enhances the passive ion permeability away from the transition, but leaves it almost unchanged at the transition.

Comparison with experiments

Lipid/cholesterol mixtures are some of the most intensively studied systems in the physical chemistry of model membranes (for a recent review, see for example Ref. 33). It is remarkable that only recently has a common consensus been reached regarding the phase equilibria in such systems [5–6] and the interpretation of the phase equilibria in terms of molecular properties [4]. Regarding the actual organization and lateral microscopic distribution of cholesterol in membranes, the situation is less clear. Most workers have concentrated on the regime of high-cholesterol contents (10–50 mol%) and there are very little data available in the region of the phase diagram (up to 10 mol%) where the phase separation effects are marginal in the case of DPPC. In this section we shall discuss our findings in this work in relation to a variety of experimental results. It should be emphasized again that the model underlying our results is only expected to be a quantitatively realistic model of cholesterol-lipid membranes for cholesterol concentrations up to about 10 mol%. Still, some of the results for higher concentrations may be qualitatively relevant for the interpretation of experiments. The model calculations were carried out for a set of model parameters pertinent to DPPC bilayers. However, we expect that the conclusions drawn will apply to phosphatidylcholine membranes in general.

Cholesterol's well-known expansion effect below the transition and condensing effect above the transition [33] are closely reproduced by Fig. 2. It should be noted that these effects may not be visible in the total membrane area, Fig. 1, due to the mere dilution effect. The total area, A, can be obtained by micromechanic measurements [34] which do not, however, lead to an absolute determination of the area. The results in Fig. 1 are in good agreement with recent measurements of relative areas of DMPC/cholesterol bilayers [34]. The area per lipid molecule, A_L, can be obtained indirectly from ^{2}H-NMR experiments which measure the first moment, M_1 of the quadrupolar splitting [5,6]. M_1 can be related approximately to the membrane thickness [35] and hence to the membrane area, assuming the membrane volume to be constant. The experimental data for M_1 vs. temperature and x_C are in qualitative accordance with the theoretical data of Fig. 2, even at high concentrations.

The lateral isothermal compressibility, $\chi(T)$, has been measured by micromechnics for DMPC/cholesterol membranes [34] and it was found that $\chi(T)$ decreases with x_C for high concentrations, in agreement with Fig. 3. The subtle effects found theoretically at low concentrations are outside the resolution limits of the present type of compressibility measurements. It should be noted that our model study in no instance shows an enhancement of the compressibility at the transition as x_C is increased. This is intimately related to our basic assumption about the cholesterol molecules being mobile (annealed dilution) in the membrane. A previous phenomenological study by Jähnig [36], who assumed that the intrinsic molecules are stationary (quenched dilution), led to an enhancement of $\chi(T_m)$ as x_C is increased, in contradiction to experimental findings [34].

It is experimentally very difficult to assess directly the presence of heterogeneous membrane structures and cluster-formation phenomena. The main evidence for cluster formation in membranes near their phase transition therefore derives from indirect measurements [8,13,37]. Specifically, Freire and Biltonen [8] have used calorimetric data to determine the cluster-distribution function without assuming a particular model of the chain-melting transition. Extrapolating this relationship to lipid-cholesterol membranes, bearing in mind the specific-heat measurements as a function of concentration for small x_C [6,38,39], we suggest that our finding of larger clusters away from the transition temperature, cf. Fig. 5, is in accordance with the experimental broadening of the specific heat for $x_C \leq 10$ mol%. For completeness, it should be noted that a theoretical description of the broad, second component of the specific heat observed experimentally at higher values of x_C requires a model which takes account of both chain-conformational as well as crystalline degrees of freedom (Ipsen, J.H., Mouritsen, O.G. and Zuckermann, M.J., unpublished data).

We are not aware of any experimental data for passive ion permeability in the low-concentration regime. For high-cholesterol concentrations, the experimental measurements show [24], in agreement with Fig. 12, that the permeability is lowered in the presence of 50 mol% cholesterol. As pointed out in our earlier work [14], the occurrence of interfacial regions in membranes may also stimulate permeation of other molecular species. The experimental finding of a lowered water

permeation in membranes containing large amounts of cholesterol [28,41] is in accordance with our results. Similarly, our qualitative results for high concentrations are in line with general expectations of cholesterol being a main molecular species to assure high mechanical coherence and low leakiness [34,35].

It was recently reported that small amounts of cholesterol enhance the mobility of certain spin-labels in membranes [42]. The enhanced mobility was related to cholesterol's ability to stabilize defect lines [43]. Our finding of an increased interfacial area in the presence of cholesterol gives further support to this interpretation. Moreover, it is interesting to note that a similar stabilization and ramification of interfacial regions due to cholesterol has been observed directly in lipid monolayers by means of epifluorescence microscopy [44].

Experimental studies of the kinetic properties of cholesterol-containing lipid bilayers in the transition region have been interpreted in terms of cluster formation [37,38]. It was then found that cholesterol at 7.5 mol% suppresses the membrane processes leading to cluster formation at the transition, but with a tendency to enhance these processes away from the transition [37]. This is in agreement with our predictions, cf. Fig. 5. At higher-cholesterol concentrations, the kinetics associated with the cooperative cluster-formation processes are strongly suppressed [37].

Some enzymatic processes associated with membranes are believed to be controlled by interfacial properties. A particularly striking example is that of pancreatic phospholipase for which it is known that hydrolysis only occurs in the transition region [30]. The rate of activation varies strongly with temperature and it changes two orders of magnitude within 1°C of the phase transition [31]. This observation has been linked to the lipid-membrane fluctuations and the formation of a particular interfacial environment which supports the active conformation of the enzyme. In the presence of cholate, which has a structure very similar to that of cholesterol, it was found [32] that small amounts of cholate strongly increase the rate of activation away from the phase transition. This is consistent with the interpretation that cholate increases the interfacial area.

Conclusions

The lipid-membrane heterogeneous structure and interfacial properties described in this paper were derived from first principles using a microscopic interaction model and a numerical computer simulation method. Similarly, the heterogeneous and highly non-random distribution discovered for intrinsic molecules such as cholesterol are not due to any initial assumption but a mere consequence of the cooperativity and lateral density fluctuations in the membrane model. The lipid-domain interfaces formed in the transition region (cf. Figs. 4, 6 and 7) are, as pointed out in our earlier work [10,14], stabilized by the intermediate lipid-chain conformations which are attracted to the interface *. Hydrophobically smooth intrinsic molecules, such as cholesterol, which have no special preference (at low concentrations) to any of the two lipid phases are also attracted to this interface. We therefore find it remarkable that the cholesterol level is about twice as high in the interfacial region as in the bulk (cf. Fig. 11). At the same time, cholesterol induces a larger and more ramified interface (cf. Fig. 6).

The physical reason for cholesterol's dramatic effects on lipid-membrane interfacial properties is that cholesterol lowers the interfacial tension for the mixed system. This may also provide an explanation of the subtle temperature-dependence of these effects, cf. Figs. 8–11, which show that the relative effect of cholesterol at low concentrations is largest away from the transition temperature and that the effect at the very transition is very small. Considering that the lipid chain-melting transition is strongly influenced by lateral density fluctuations of a type which gives rise to pseudo-critical phenomena [11], which in turn lower the interfacial tension, one would expect that, close to the pseudo-critical point, intrinsic molecules would have little effect on the membrane heterogeneity, in accordance with our findings. Obviously, this explanation is only appropriate at low concentrations, where the strong lateral density fluctuations remain independent of cholesterol content, cf. Fig. 3.

The various results presented in this paper suggest that there are a number of interesting interfacial properties and fluctuation phenomena induced in lipid membranes by small amounts of cholesterol, and that it may be worthwhile extending the experimental carefully studied concentration regime, of, for example, passive ion permeability, to include concentrations below 10 mol%, where the effects due to lateral phase separation are negligible.

Acknowledgements

This work was supported by the Danish Natural Science Research Council under Grant J. Nr. 5.21.99.72. L.C.-H. acknowledges the support of the C. Gulbenkian Foundation, Lisbon, Portugal and of the Danish Research Council for Scientific and Industrial Research. It is a pleasure for the authors to acknowledge very stimulating discussions with Rodney Biltonen, Myer Bloom, and Martin Zuckermann.

* The lack of intermediate states in the early study [18] by computer simulation techniques of a two-state model of lipid/cholesterol mixtures is likely to be the main reason for the failure of that study to faithfully describe those mixtures.

References

1 Sackmann, E. (1983) in Biophysics (Hoppe, W., Lohmann, W., Markl, H. and Ziegler, H., eds.), pp. 425–457, Springer, Heidelberg.
2 Abney, J.R. and Owicki, J.C. (1985) in Progress in Protein–Lipid Interactions (Watts, A. and De Pont, J.J.H.H.M., eds.), pp. 1–60, Elsevier, Amsterdam.
3 Sperotto, M.M. and Mouritsen, O.G. (1989) Cell Biophys., in press.
4 Ipsen, J.H., Karlström, G., Mouritsen, O.G., Wennerström, H. and Zuckermann, M.J. (1987) Biochim. Biophys. Acta 905, 162–172.
5 Davis, J.H. (1988) in Proceedings of the International School of Physics 'Enrico Fermi' on Medical Applications of NMR, Varenna, (Maraviglia, B., ed.), pp. 302–312, North-Holland, Amsterdam.
6 Vist, M.R. (1984) MSc. Thesis, University of Guelph, Ontario, Canada.
7 Mortensen, K., Pfeiffer, W., Sackmann, E. and Knoll, W. (1988) Biochim. Biophys. Acta 945, 221–245.
8 Freire, E. and Biltonen, R. (1978) Biochim. Biophys. Acta 514, 54–68.
9 Doniach, S. (1978) J. Chem. Phys. 68, 4912–4916.
10 Mouritsen, O.G. (1983) Biochim. Biophys. Acta 731, 217–221.
11 Mouritsen, O.G. and Zuckermann, M.J. (1985) Eur. Biophys. J. 12, 75–86.
12 Genz, A. and Holzwarth, J.F. (1986) Eur. Biophys. J. 13, 323–330.
13 Ruggiero, A. and Hudson, B. (1988) Biophys. J., in press.
14 Cruzeiro-Hansson, L. and Mouritsen, O.G. (1988) Biochim. Biophys. Acta 944, 63–72.
15 Mouritsen, O.G. (1984) Computer Studies of Phase Transitions and Critical Phenomena, Springer, Heidelberg.
16 Pink, D.A., Green, T.J. and Chapman, D. (1980) Biochemistry 19, 349–356.
17 Caillé, A., Pink, D.A., De Verteuil, F. and Zuckermann, M.J. (1980) Can. J. Phys. 58, 581–611.
18 Mouritsen, O.G., Boothroyd, A., Harris, A., Jan, N., Lookman, T., MacDonald, L., Pink, D.A. and Zuckermann, M.J. (1983) J. Chem. Phys. 79, 2027–2041.
19 Pink, D.A. and Carroll, C.E. (1978) Phys. Lett. 66A, 157–160.
20 Pink, D.A., Green, T.J. and Chapman, D. (1981) Biochemistry 20, 6692–6698.
21 Pink, D.A., Lookman, T., MacDonald, A.L., Zuckermann, M.J. and Jan, N. (1982) Biochim. Biophys. Acta 687, 42–56.
22 Zuckermann, M.J. and Mouritsen, O.G. (1987) Eur. Biophys. J. 15, 77–86.
23 Engelman, D.M. and Rothman, J.E. (1972) J. Biol. Chem. 247, 3694–3697.
24 Papahadjopoulos, D., Jacobsen, K., Nir, S. and Isac, T. (1973) Biochim. Biophys. Acta 311, 330–348.
25 Georgallas, A., MacArthur, J.D., Ma, X.-P., Nguyen, C.V., Palmer, G.R., Singer, M.A. and Tse, M.Y. (1987) J. Chem. Phys. 86, 7218–7226.
26 Tsong, T.Y. (1975) Biochemistry 14, 5415–5417.
27 Kanehisa, M.I. and Tsong, T.Y. (1978) J. Am. Chem. Soc. 100, 424–432.
28 Carruthers, A. and Melchior, D.L. (1983) Biochemistry 22, 5797–5807.
29 March, D., Watts, A. and Knowles, P.F. (1976) Biochemistry 15, 3570–3578.
30 Op den Kamp, J.A.F., Kauertz, M.T. and Van Deenen, L.L.M. (1975) Biochim. Biophys. Acta 406, 169–177.
31 Menashe, M., Romero, G., Biltonen, R.L. and Lichtenberg, D. (1986) J. Biol. Chem. 261, 5328–5333.
32 Gheriani-Gruszka, N., Almog, S., Biltonen, R.L. and Lichtenberg, D. (1988) J. Biol. Chem. 263, 11808–11813.
33 Presti, F.T. (1985) in Membrane Fluidity in Biology (Aloia, R.C. and Boggs, J.M., eds.), pp. 97–146, Academic Press, New York.
34 Needham, D., McIntosh, T.J. and Evans, E. (1988) Biochemistry 27, 4668–4673.
35 Bloom, M. and Mouritsen, O.G. (1988) Can. J. Chem. 66, 706–712.
36 Jähnig, F. (1981) Biophys. J. 36, 347–357.
37 Genz, A. and Holzwarth, J.F. (1986) Biophys. J. 50, 1043–1051.
38 Blume, A. and Hillmann, M. (1986) Eur. Biophys. J. 13, 343–353.
39 Mabrey, S., Mateo, P.L. and Sturtevant, J.M. (1978) Biochemistry 17, 2464–2468.
40 Estep, T.N., Mountcastle, D.B., Biltonen, R.L. and Thompson, T.E. (1978) Biochemistry 17, 1984–1989.
41 Blok, M.C., Van Deenen, L.L.M. and De Gier, J. (1977) Biochim. Biophys. Acta 464, 509–518.
42 Subczynski, W.K. and Kusumi, A. (1986) Biochim. Biophys. Acta 854, 318–320.
43 Sackmann, E., Rüppel, D. and Gebhardt, C. (1980) in Liquid Crystals of One- and Two-Dimensional Order (Helfrich, W. and Heppke, G., eds.), pp. 309–326, Springer, Berlin.
44 Veis, R.M. and McConnell, H.M. (1985) J. Phys. Chem. 89, 4453–4459.